Lower critical solution coexistence curve and physical properties (density, viscosity, surface tension, and interfacial tension) of 2,6-lutidine + water

ARTICLE *in* JOURNAL OF CHEMICAL & ENGINEERING DATA · OCTOBER 1993

Impact Factor: 2.04 · DOI: 10.1021/je00012a008

4 AUTHORS, INCLUDING:

Carlos A. Grattoni
University of Leeds
87 PUBLICATIONS **713** CITATIONS
SEE PROFILE

Richard A. Dawe
The University of the West Indies, Trinidad a…
140 PUBLICATIONS **1,450** CITATIONS
SEE PROFILE

Physical Properties (Density, Viscosity, Surface Tension, Interfacial Tension, and Contact Angle) of the System Isopropyl Alcohol + Cyclohexene + Water

Yahya M. Al-Wahaibi,*,† Carlos A. Grattoni,‡ and Ann H. Muggeridge§

Department of Petroleum and Chemical Engineering, Sultan Qaboos University, Alkhod 123, Muscat, Oman, School of Earth and Environment, University of Leeds, Leeds LS2 9JT, U.K., and Department of Earth Science and Engineering, Imperial College, London SW7 2AZ, U.K.

The equilibrium physical property data (densities, viscosities, refractive index, interfacial tensions, and contact angles) for the liquid−liquid system isopropyl alcohol + cyclohexene + water have been determined at 294 K. The phase diagram and equilibrium tie lines were evaluated. The compositions of the coexistence curve were determined through the refractive index, densities were determined by an electronic oscillating U-tube densitometer, viscosities were determined by a U-tube viscometer, surface/interfacial tensions were determined by a du Noüy ring and a spinning drop method, and contact angles were determined with a goniometer contact angle meter.

Introduction

In recent work[1−3] examining mechanisms of oil recovery via immiscible and multi-contact miscible displacements within heterogeneous porous media, use was made of a three-component two-phase liquid−liquid system, namely, isopropyl alcohol (IPA) + cyclohexene + water (denoted as ICW throughout this paper). This system exhibits a critical point (55.3 % IPA concentration, 29.2 % water concentration, 15.5 % cyclohexene concentration) at ambient temperature and pressure.[1−3] This fact together with other physical properties described in this paper make it ideal for studying multi-phase flow through porous media.

On enriching the immiscible water + cyclohexene phases with IPA, the alcohol partitions into two phases, A and B, with compositions C_A and C_B, respectively. The equilibrium phase diagram for the system is shown in Figure 1. Phase A is rich in water (termed the water-rich phase); phase B is rich in cyclohexene (termed the cyclohexene-rich phase). Any composition on the tie line between phases A and B will separate into these two phases provided the temperature remains constant. The relative amount of each phase (A and B phase fractions) is controlled by the choice of the initial composition.[4] Thus, by changing the initial fluid composition *C*, within a given tie line, the complete phase fraction range (from 100 % phase A to 100 % phase B) can be obtained. The equilibrated ICW liquid system has uniquely defined physical properties (density, interfacial tension, etc.) that can be readily varied in a systematic manner by changing the IPA concentration. This is especially useful for studying flow phenomena where interfacial tensions, viscosities, and densities need to be varied in a systematic and controlled manner. This paper presents results of refractive index (RI), density (ρ), viscosity (η), surface tension, interfacial tension (σ), and contact angles of the equilibrated phases within the two-phase region of the ICW system at 294 K and ambient pressure.

* Corresponding author e-mail: ymn@squ.edu.om.
† Sultan Qaboos University.
‡ University of Leeds.
§ Imperial College.

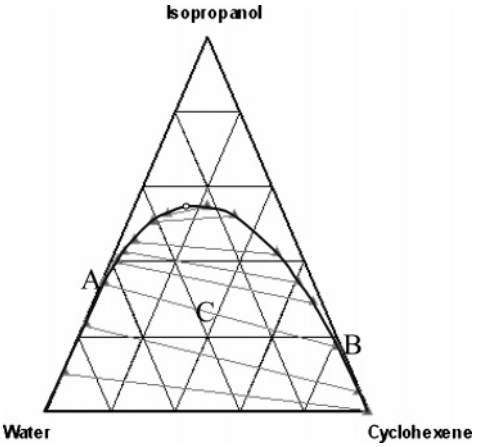

Figure 1. IPA + water + cyclohexene ternary diagram at 294 K and atmospheric pressure.

Experimental Section

Materials. The isopropyl alcohol ($(CH_3)_2CHOH$) and cyclohexene (C_8H_{10}) were both supplied by VWR International with purities of 99.7 % and 99.0 %, respectively, and were used without further preparation. The water used had been singly distilled. The purities of the fluids were sufficient for the determination of the system's phase separation and physical property behavior at ambient pressure and temperature described in this work.

Previous Data. The coexistence curve of the ICW system was first published by Washburn et al.[5] in 1940. Coexistence curve data were provided at temperatures of (289, 294, and 299) K. They also provided RI data for equilibrated solutions at these temperatures. However, no data were measured at 294 K.

Washburn et al. found that increasing the temperature caused a noticeable change in the slopes of the tie lines for the ICW system. For example, the plait point at 289 K was not far from the highest point of the solubility curve, while at 299 K it was further down on the water-rich side of the curve. They experienced experimental difficulties in obtaining the plait point at the highest temperature of 309 K; nevertheless, they observed that at this temperature it is still farther down on the water-rich

10.1021/je060442b CCC: $37.00
Published on Web 02/20/2007

Table 1. Total Composition of the Mixtures within the Two-Phase Region (mixtures 1 to 6) and Single-Phase Region (mixture 7) at 294 K and Atmospheric Pressure

	components % (v/v)		
mixture	IPA	water	cyclohexene
1	0.0	50.0	50.0
2	16.0	42.0	42.0
3	28.0	36.0	36.0
4	36.0	32.0	32.0
5	44.0	28.0	28.0
6	50.0	25.0	25.0
7	55.6	22.2	22.2

side of the curve. However, increasing the temperature from (289 to 309) K caused very little change in the area in which conjugate solutions were found. The area was slightly larger at the lowest temperature.

Methods. The physical properties (densities, viscosities, refractive index, interfacial tensions and contact angles) of seven different ICW mixtures were investigated. Mixtures 1−6 were in the two-phase region, and mixture 7 was in the single-phase region. The compositions of these mixtures are shown in Table 1. The mixtures were prepared by measuring the required amount of each component (by volume) and shaking the mixture by hand. The phases were then left to equilibrate. The phases segregated in times that ranged from minutes to 1 day (depending on the interfacial tension between pairs of phases; low IFT mixtures took longer to separate). In the remainder of this paper, the mixtures will be referred by their phase IPA concentrations (knowing the IPA concentration in each phase, concentrations of cyclohexene and water can be determined using Table 2).

Results and Discussion

Refractive Index. Phase compositions were analyzed by RI as each equilibrated phase was found to have a unique value. The RI measurements were made using a Bellingham and Stanley Abbe 60 instrument (sodium D1 line), precise to 0.0002. The refractometer was calibrated with water before each use. First, the surface of the refractometer prism was cleaned using ethanol and a lens wiper. This ensured that no stains or air bubbles were left on the prism surface. Next several drops of distilled water were placed on the prism surface using a plastic syringe and covered with a cap. The RI of the distilled water was then measured at 294 K. The RI of the distilled water was found to be 1.33 ± 0.005, which agrees well with the value reported in the literature.

The RI data of all the phases resulting from the seven mixtures covering the single- and two-phase composition range were measured at 294 K and atmospheric pressure. The results are presented in Table 2. Care was required when drawing samples of each phase in a given mixture into the syringe to avoid contamination with the other phase.

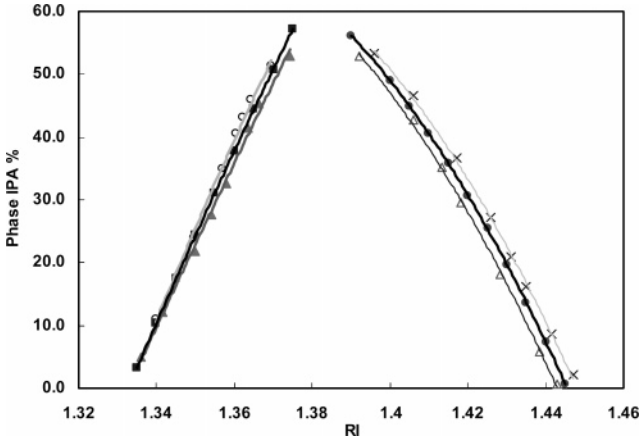

Figure 2. IPA concentrations as a function of refractive index at different temperatures in the equilibrated upper and lower phases (error: ± 0.5 %): ×, cyclohexene-rich phase at 289 K; ●, cyclohexene-rich phase at 294 K; △, cyclohexene-rich phase at 299 K; ▲, water-rich phase at 289 K; ■, water-rich phase at 294 K; ○, water-rich phase at 299 K.

The data relating IPA concentration (*IPA*) to the refractive index (*Ri*) of the water- and cyclohexene-rich phases at different temperatures (289, 294, and 299 K) were fitted with empirical equations (see Figure 2). The RI data at (289 and 299) K were taken from Washburn et al.[5] while the RI data at 294 K were measured in this study as described above.

The fitted curves in Figure 2 are all polynomial of the form:

$$\mathrm{IPA} = -A(Ri)^2 + B{\cdot}Ri - C \quad (1)$$

where the constants *A*, *B*m and *C* are listed in Table 3. In order to determine the concentrations of the water component in the water- and cyclohexene-rich phases, two more equations (eqs 2 and 3) were developed using equilibrium IPA−water relationships for each equilibrated phase, as shown in Figure 3. Equation 2 relates IPA concentrations (IPA_w) with the water concentrations (W_w) in the water-rich phase whereas eq 3 relates (IPA_c) with the water concentrations (W_c) in the cyclohexene-rich phase. Based on the definition of component fraction for a phase (i.e., concentrations of all components in a phase should sum up to one), concentrations of the cyclohexene component in each phase were calculated (see Table 2):

$$\mathrm{IPA_w} = 1.0734(W_w^3) - 2.6184(W_w^2) + 1.1327(W_w) + 0.4161 \quad (2)$$

$$\mathrm{IPA_c} = 0.13[\ln(W_c)] + 0.768 \quad (3)$$

The refractive indices measured at 294 K as a function of the % (v/v) of IPA in water- and cyclohexene-rich phases for the mixtures tested are presented in Figure 4. Since miscibility can be achieved by increasing the concentration of IPA in the

Table 2. Refractive Index and Concentrations of Isopropyl Alcohol (IPA), Water (W), and Cyclohexene (C) in the Equilibrated Phases at 294 K and Atmospheric Pressure

total	RI		IPA concentration %		water concentration %		cyclohexene concentration %	
IPA %	C-rich	W-rich	C-rich	W-rich	C-rich	W-rich	C-rich	W-rich
0.0	1.44737	1.33388	0.00	0.00	0.00	100.00	100.00	0.00
16.0	1.44517	1.35204	1.04	27.04	0.50	72.70	98.46	0.27
28.0	1.42927	1.36101	21.07	39.05	1.72	59.23	77.21	1.72
36.0	1.41783	1.36408	33.49	43.08	2.51	53.54	64.01	3.37
44.0	1.40614	1.36951	44.45	47.00	6.87	47.21	48.68	5.79
50.0	1.39930	1.37200	50.06	50.07	11.51	41.59	38.43	8.34
55.6	1.3850		55.60		22.20		22.20	

Table 3. Constants A, B, and C Values for Different Temperatures (*T*) Generated by Fitting the Data in Figure 2 to a Quadratic Equation (eq 1)[a]

T	oil phase			gas phase		
K	*A*	*B*	*C*	*A*	*B*	*C*
289	1047.10	4130.90	3645.40	6475.99	17386.82	11597.80
294	2151.30	7176.00	5742.60	6377.90	17073.00	11352.00
299	3255.40	10221.00	7839.70	6279.81	16759.00	11107.00

[a] Values obtained for temperatures 289 and 299 K are from Washburn et al.[5] The values were obtained at atmospheric pressure.

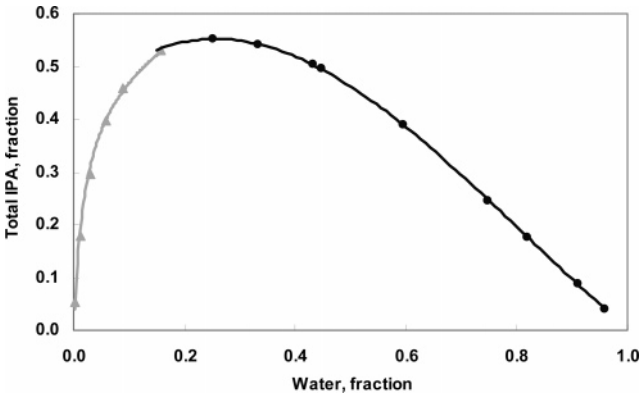

Figure 3. IPA concentrations vs water concentrations in water- and cyclohexene-rich phases at 294 K and atmospheric pressure: ●, water-rich phase; ▲, cyclohexene-rich phase.

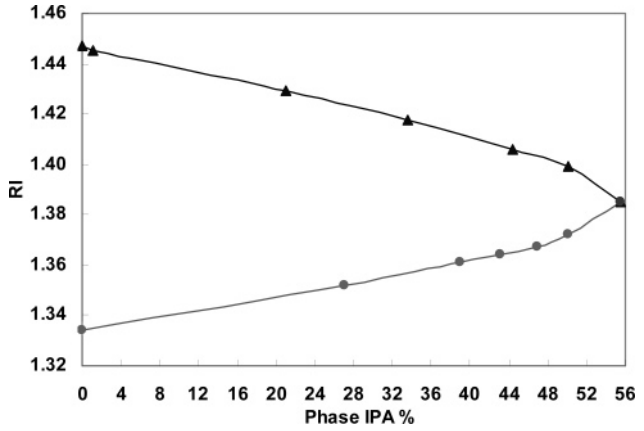

Figure 4. Equilibrated phase refractive indices as a function of phase IPA concentration measured at 294 K and atmospheric pressure (error: ± 0.5 %): ●, water-rich phase; ▲, cyclohexene-rich phase.

system, all properties of the equilibrated phases are plotted against the concentrations of IPA in each equilibrated phase.

Phase Behavior. The equilibrated phase compositions for each of the seven mixtures were plotted on the equilibrium ternary diagram originally determined by Washburn et al.[5] (see Figure 1). It can be concluded that the tie line data of Washburn et al. compare favorably with those presented here. Discrepancies between the two sets of data are consistent with small differences in specimen purities and experimental error.

The critical point (55.3 % IPA concentration, 29.2 % water concentration, 15.5 % cyclohexene concentration) was determined by noting the highest IPA concentration at which phase separation occurred and confirming this by extrapolation of the phase diagram (Figure 1). This was also confirmed by preparing a mixture of ICW (with 55.6 % IPA concentration, 22.2 % water concentration, and 22.2 % cyclohexene concentration) just higher than that at the critical point. This mixture formed a single phase whose properties are discussed in detail in subsequent sections of this paper.

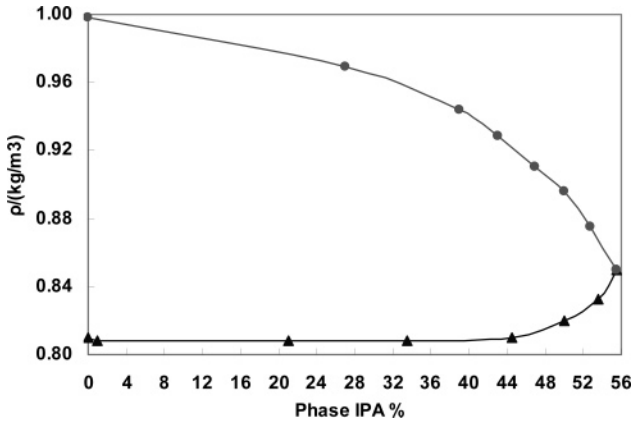

Figure 5. Equilibrated phase densities (ρ) as a function of phase IPA concentrations at 294 K and atmospheric pressure (error: ± 0.5 %): ●, water-rich phase; ▲, cyclohexene-rich phase.

Table 4. Densities ρ and Viscosities η for the Equilibrated Phases from the Seven Mixtures Listed in Table 1 (error: ± 0.5 %) at 294 K and Atmospheric Pressure

	ρ/kg·m^{-3}		η/mPa·s	
total IPA %	C-rich	W-rich	C-rich	W-rich
0.0	0.81	0.99	0.67	1.03
16.0	0.81	0.97	0.68	2.58
28.0	0.81	0.94	0.76	3.30
36.0	0.81	0.93	0.98	3.60
44.0	0.81	0.91	1.55	3.62
50.0	0.82	0.89	1.84	3.70
55.6	0.850		3.10	

Density. The density (ρ) of each phase, at atmospheric pressure, was measured to an accuracy of ± 0.1 kg·m^{-3} using an Anton Paar DMA48 density meter calibrated with water and air according to the manufacturer's instructions. The principle of measurement is to monitor the variation in frequency of a fluid-filled vibrating U-tube caused by changes in its mass.

In order to prevent contamination between different phases, before each measurement the measuring cell was carefully cleaned by rinsing it with at least 5 mL of methylated spirits. Then dry air was passed through the measuring cell for at least 10 min to evaporate any remaining liquid.

As shown in Figure 5, the densities in the cyclohexene-rich phase remained almost constant for low concentrations of IPA and only started to increase at 45 % IPA (knowing one component concentration and using Table 2, concentrations of the other two components can be determined). On the other hand, the water-rich phase density decreased gradually. The water- and cyclohexene-rich phase densities converged to a single value at the critical point (55.3 % IPA concentration, 29.2 % water concentration, 15.5 % cyclohexene concentration). This was confirmed by measuring the density of the mixture with an IPA concentration of 55.6 % (i.e., just slightly higher than that at the critical point). All the density measurements are presented in Table 4.

Viscosity. The viscosity (η) of each phase was measured using a U-tube (Ubbelohde) viscometer. The standard fluid viscosity was water, with values taken from standard tables and the densities determined by densitometer as described earlier. The accuracy was estimated to be within ± 0.05 mPa·s.

The viscosities of the equilibrated phases were determined according to the following equation:

$$\frac{\eta_1}{\eta_2} = \frac{\rho_1 t_1}{\rho_2 t_2} \tag{4}$$

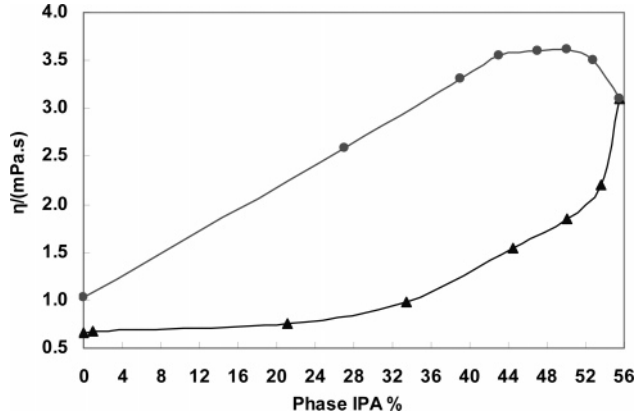

Figure 6. Equilibrated phase viscosities (η) as a function of phase IPA concentration at 294 K and atmospheric pressure (error: ± 0.5 %): ●, water-rich phase; ▲, cyclohexene-rich phase.

Table 5. Surface Tensions for the Water-Rich Phase, Interfacial Tensions σ for the Equilibrated Phases (mixtures shown in Table 1), and Contact Angles between Liquid Phases and Silica Surface at 294 K and Atmospheric Pressure

total IPA %	surface tension for W-rich / mN·m^{-1}	s / mN·m^{-1}	contact angle / deg ($\theta \pm 1$)
0.0	27.2	24.2	
16.0	26.7	6.9	48
28.0	25.4	1.5	47
36.0	25.2	0.6	
44.0	25.1	0.1	35
50.0	24.9	0.03	5

where η is the fluid viscosity (Pa·s); ρ is the fluid density (kg·m^{-3}); t is the time taken to flow through the capillary tube (s); and the subscripts 1 and 2 refer to pure water and the fluid of unknown viscosity, respectively. The reference fluid is water, with its viscosity taken from standard tables and the densities of both fluids determined by densitometer, as described in the previous section. The accuracy of this method is estimated to be within ± 0.1 mPa·s.

Figure 6 shows how the viscosities of the water- and cyclohexene-rich phases vary as a function of IPA concentration. It can be clearly seen that viscosities of the two phases do not converge as fast as other properties.

In particular, the viscosity of the water-rich phase was found to undergo abnormal behavior near the critical condition. The viscosity of this phase was found to be higher than the viscosity of any of the components. The reason behind this phenomenon may be due to hydrogen bonding between the IPA and the water.[6] As the mixture becomes enriched with IPA, hydrogen bonding is more likely to occur, resulting in an increase in the mixture viscosity until a maximum is reached. After this point the viscosity decreases, as there are fewer water molecules available for hydrogen bonding. Ultimately the viscosity converged with that of the cyclohexene-rich phase to a single value at the critical point. Table 4 presents the viscosity measurements for water- and cyclohexene-rich phases for all of the samples.

Surface and Interfacial Tension. The surface tensions of the equilibrated water-rich phase and the IFTs between equilibrated water- and cyclohexene-rich phases were measured using the du Noüy ring method on a Krüss K10 (Hamburg) automatic tensiometer with an accuracy of ± 0.5 mN·m^{-1}. The ring method was chosen because (i) it is suitable for both surface (gas−liquid) and interfacial (liquid−liquid) tensions measurement; (ii) it is virtually independent of wetting angle; and (iii) it gives an extremely accurate, easily reproducible measurement. The surface tensions of the water-rich phase and the IFT between equilibrated phases are given in Table 5.

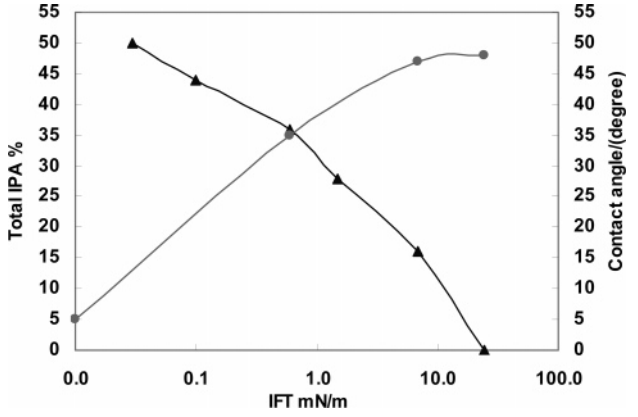

Figure 7. Total IPA concentration as a function of the interfacial tensions (σ) between the equilibrated phases and contact angles between the phases and a silica surface at 294 K and atmospheric pressure (error: ± 0.5 %): ●, contact angle; ▲, total IPA %.

The IFTs studied ranged from 24.2 mN·m^{-1} to 0.03 mN·m^{-1}. Note that the IFT's (0.1 and 0.03) mN·m^{-1} were measured using a Kruss Site04 spinning drop tensiometer, which can be used for IFT measurements over the range from (1.0 to 10^{-6}) mN·m^{-1}.[7] This range included all the mixtures within the two-phase region of the ICW system. Figure 7 illustrates the relationship between the IFT and total IPA concentration for the equilibrated phases. The IFT decreases as the IPA concentration increases until it reaches zero when the phases become miscible at the critical point.

Contact Angles. The contact angle is a measure of the relative strength of adhesion of two fluids toward a solid. It has a major influence on the hydrocarbon−water distribution and flow within porous media, and it is a measure of the wettability of the system.[8] The equilibrium contact angle for the coexisting phases (measured through the water-rich phase) and a flat silica glass slide were measured using an Erma (goniometer type) contact angle meter. The results are given in Table 5.

Figure 7 shows also the relationship between contact angle and interfacial tension. As shown in Figure 7, the contact angle has a small variation at high gas−oil interfacial tensions above 8 mN·m^{-1} and then decreases rapidly approaching zero at the critical point. A similar trend for a different system (naturally occurring hydrocarbon system) was previously reported by Al-Siyabi et al.[9]

Summary

The equilibrium phase diagram and physical properties for a three-component two-phase (liquid−liquid) IPA + water + cyclohexene fluid system have been measured. Tables 1 and 2 summarize the composition of the equilibrated phases and the RI of the mixtures investigated within the single- and two-phase regions. Tables 4 and 5 present densities, viscosities, surface tensions, and interfacial tensions of the equilibrated phases. Equilibrium contact angles between the liquid phases and a silica slide are summarized in Table 5.

Acknowledgment

The authors thank Dr. Alex Bismark (Imperial College, London) for the use of the spinning drop tensiometer.

Literature Cited

(1) Al-Wahaibi, Y. M.; Muggeridge, A. H.; Grattoni, C. A. Experimental and numerical studies of gas/oil multicontact miscible displacements in homogeneous porous media. *Proceedings of the SPE Reservoir Simulation Symposium*, Houston, TX, 2005 (SPE 92887).

(2) Al-Wahaibi, Y. M.; Muggeridge, A. H.; Grattoni, C. A. The effect of cross-bedding laminations on the efficiency of gas/oil multi-contact miscible displacements. *Proceedings of the 14th Europec Biennial Conference*, Madrid, 2005 (SPE 94135).

(3) Al-Wahaibi, Y. M.; Muggeridge, A. H.; Grattoni, C. A. Gas/oil nonequilibrium in multicontact miscible displacements within homogeneous porous media. *Proceedings of the 18th SPE/DOE Symposium on Improved Oil Recovery*, Tulsa, OK, 2006 (SPE 99727).

(4) Francis, A. W. *Liquid−Liquid Equilibriums*; Interscience: New York, 1963.

(5) Washburn, E. R.; Graham, C. L.; George, B. A.; Laurence, F. T. The ternary systems involving cyclohexene, water, and methyl, ethyl, and isopropyl alcohols. *J. Am. Chem. Soc.* **1940**, *62*, 1454−1457.

(6) Grattoni, C. A.; Dawe, R. A.; Yen, C. S.; Gray, J. D. Lower critical solution coexistence curve and physical properties (density, viscosity, surface tension, and interfacial tension) of 2,6-lutidine + water. *J. Chem. Eng. Data* **1993**, *38*, 516−519.

(7) Coucoulas, L. M.; Dawe, R. A.; Mahers, E. G. The refraction correction for the spinning drop interfacial tensiometer. *J. Colloid Interface Sci.* **1983**, *93*, 281−284.

(8) Adamson, A. W. *Physical Chemistry of Surfaces*; John Wiley and Sons: New York, 1982.

(9) Al-Siyabi, Z.; Danesh, A.; Tohidi, B.; Todd, A. C. Variations of gas−oil−solid contact angle with interfacial tension. *Pet. Geosci.* **1999**, *5*, 37−40.

Received for review October 8, 2006. Accepted December 28, 2006. Y.M.A.-W. thanks Sultan Qaboos University for their financial support throughout this project.

JE060442B